PIEZOELECTRIC ENERGY HARVESTING FROM AEROELASTIC VIBRATION WITH COMPOSITE PLATE WINGS

Masaki KAMEYAMA[+1] and Kanjuro MAKIHARA[+2]
[+1]Department of Mechanical Systems Engineering, Shinshu University, Nagano, JAPAN
[+2]Department of Aerospace Engineering, Tohoku University, Sendai, JAPAN

The present paper treats the piezoelectric energy harvesting from aeroelastic vibration with cantilevered laminated plates. The aeroelastic flutter energy harvester is composed of a piezoelectric patch attached to the structures and a conventional harvesting circuit. A diode bridge of four diodes is connected to the piezoelectric patch and it provides a mechanism of current rectification. Aeroelastic analysis of composite plate wings with a piezoelectric patch is based on the finite element method and the subsonic unsteady lifting surface theory. The effect on location of piezoelectric patch on converged voltage in the harvesting system is examined through the numerical examples.

Keyword: Energy Harvesting, Subsonic Flutter, Piezoelectrics, Composite Materials

1. INTRODUCTION

Aeroelastic characteristics have played the significant role in structural design. Flutter is one of the representative dynamic phenomena of aeroelastic instability, which results in catastrophic destruction of structures. Although flutter is recognized as a harmful phenomenon from the viewpoint of structural integrity, it can be conversely utilized as profitable energy source for vibration-based energy harvesting. So far, a lot of research on energy harvesting from aeroelastic vibration has been carried out[1-10].

The present paper treats the piezoelectric energy harvesting from aeroelastic vibration with cantilevered laminated plates. Aeroelastic analysis of composite plate wings with a piezoelectric patch is based on the finite element method and the subsonic unsteady lifting surface theory. The effect on location of piezoelectric patch on converged voltage in the harvesting system is examined through the numerical examples.

2. FUNDAMENTAL EQUATIONS[11)]

The aeroelastic flutter energy harvester is composed of a piezoelectric patch attached to the structures and a harvesting circuit as shown in Fig. 1(a) and 1(b), respectively. A diode bridge of four diodes is connected to the piezoelectric patch and it provides a mechanism of current rectification. The finite element equations for aeroelastic response of cantilevered laminated plates with a piezoelectric patch can be described as follows[12)]:

$$[M]\{\ddot{w}(t)\}+[C]\{\dot{w}(t)\}+[K]\{w(t)\}+\{\Theta\}V_p(t)=q[Q]\{w(t)\}, \tag{1}$$

$$-\{\Theta\}^T\{\dot{w}(t)\}+C_p\dot{V}_p(t)=-i(t), \tag{2}$$

where the mass, damping and stiffness matrices are denoted by M, C and K, respectively, the nodal displacement vector is denoted by $w(t)$ and the dynamic pressure is denoted by q. The aerodynamic influence matrix is denoted by Q, which can be expressed by using the Mach number and the reduced frequency defined as

$$k=\frac{b\omega}{U}, \tag{3}$$

[+1]kameyama@shinshu-u.ac.jp, [+2]makihara@ssl.mech.tohoku.ac.jp

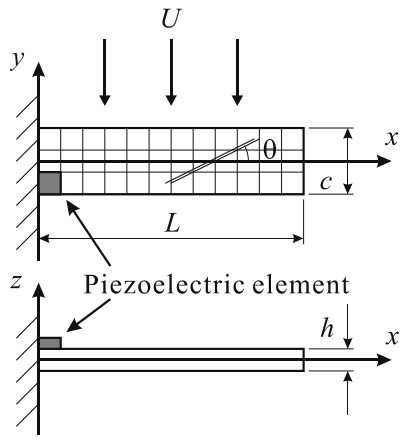

(a) Cantilevered laminated plates (L = 360 mm, $c = 2b$ = 90 mm, h = 1 mm).

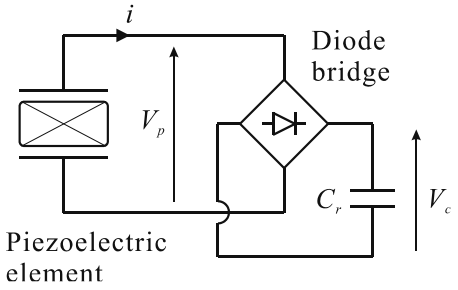

(b) Conventional harvesting circuit.

Figure 1: Schematic of aeroelastic flutter energy harvester.

where the semi-chord length at the wing root, angular frequency and free stream velocity are denoted by b (= c/2), ω and U, respectively. In this research, the aerodynamic influence matrix Q, which represents the unsteady aerodynamic forces acting on the vibratory wing surface in subsonic flow, is evaluated based on the doublet point method[13].

Amplitudes of pressure distributions on oscillatory lifting surfaces, and of their upwash velocity are related by integral equation as follows:

$$\overline{w}(x_u, y_u) = \frac{1}{8\pi} \iint_S \Delta p(\xi_d, \eta_d) Ke(x_u - \xi_d, y_u - \eta_d) d\xi_d d\eta_d \ , \tag{4}$$

where the non-dimensional amplitudes of upwash velocity and pressure differential is denoted by $\overline{w}$ and Δp, respectively. The kernel function is denoted by Ke. A doublet point, where the acceleration potential is placed, is located at (ξ_d, η_d). An upwash point, where the normal velocity of the upwash is placed, is located at (x_u, y_u). The lifting surface is assumed to lie in the place z = 0. The symbol S denotes the region of the wing area. The wing planform is divided into panel segments called element surfaces and each element surface is constructed such that the two side edges are parallel to the free stream. A doublet point and an upwash point are located on each element surface. Then the above integral equation is discretized into linear algebraic equations and the aerodynamic influence matrix Q can be evaluated.

As the doublet points of aerodynamic elements are different from the structural nodal points, it is necessary to convert the aerodynamic loading acting on the doublet points of aerodynamic element to the nodal forces of finite element. This interpolation was performed by the surface spline method[14].

Besides, the effective piezoelectric coefficient vector and capacitance are denoted by Θ and C_p, the voltage across the piezoelectric patch is denoted by $V_p(t)$ and the current flowing into a harvesting circuit is denoted by $i(t)$, which is related to the rectified voltage $V_c(t)$ by

$$i(t)=\begin{cases} C_r\dot{V}_c & if \quad V_p = V_c \\ -C_r\dot{V}_c & if \quad V_p = -V_c \\ 0 & if \quad |V_p| < V_c \end{cases}, \tag{5}$$

where the storage capacitance is denoted by C_r.

When a modal approach is introduced, the following equation can be obtained by the modal transformation ($w = \Phi w_m$) for Eqs. 1 and 2:

$$[I]\{\ddot{w}_m(t)\}+[C_m]\{\dot{w}_m(t)\}+[\Omega]\{w_m(t)\}+[\Phi]^T\{\Theta\}V_p(t)=q[Q_m]\{w_m(t)\}, \tag{6}$$

$$-\{\Theta\}^T[\Phi]\{\dot{w}_m(t)\}+C_p\dot{V}_p(t)=-i(t), \tag{7}$$

$$[Q_m]=[\Phi]^T[Q][\Phi], \tag{8}$$

where the matrix with free-vibration eigenvalues on the diagonal and the corresponding modal matrix are denoted by Ω and Φ, respectively, and modal damping matrix is denoted by C_m. The identity matrix is denoted by I.

It is necessary to transform the equations of motion into the linear time-invariant (abbreviated to LTI) state-space form for the piezoaeroelastic analysis, and the unsteady aerodynamic forces should be approximated in terms of rational functions of Laplace variable. In this research, the minimum state method[15] combined with optimization technique is adopted for the rational function approximation. The minimum state method approximates the aerodynamic influence matrix by

$$[\overline{Q}_m(\bar{s})]=[Q_0]+[Q_1]\bar{s}+[Q_2]\bar{s}^2+[D](\bar{s}[I]-[R])^{-1}[E]\bar{s}, \tag{9}$$

where the non-dimensional Laplace variable ($= sb/U$) is denoted by $\bar{s}$, semi-chord length at the wing root, free stream velocity and the Laplace variable are denoted by b, U and s, respectively. Physically, Q_0, Q_1 and Q_2 capture the dependence of the unsteady aerodynamics on displacement, velocity and acceleration, respectively. The last term in the right hand side of Eq. 9 captures the lag in the construction of aerodynamic forces associated with the circulatory effects. Here the coefficient matrices Q_0, Q_1, Q_2, D, R and E are unknown. The components of diagonal matrix R are negative constants that are selected arbitrarily. For a given R matrix, the other unknown coefficient matrices are determined by using iterative, nonlinear least-square method. Then the minimization problem of the overall least-square errors for the rational function approximation of the aerodynamic influence matrix can be stated as follows:

$$\text{[objective]} \quad \min \sum_{i,j} \sqrt{\sum_{l=1}^{nk} \left\{ \frac{\left| Q_{m,ij}(ik_l) - \overline{Q}_{m,ij}(ik_l) \right|}{\max\left(\max_l \left(\left| Q_{m,ij}(ik_l) \right| \right), 1 \right)} \right\}^2}, \tag{10a}$$

$$\text{[constraints]} \quad r_{ir} < 0 \quad (ir = 1, \ldots, nr), \tag{10b}$$

$$\text{[design variables]} \quad r_{ir} \quad (ir = 1, \ldots, nr), \tag{10c}$$

where a tabulated reduced frequency is denoted by k_l (l = 1,…,nk), tabular and approximate values of the aerodynamic influence coefficient at a specified value of reduced frequency are denoted by $Q_{m,ij}$ and $\overline{Q}_{m,ij}$,

respectively, and a diagonal component of the matrix R is denoted by r_{ir}. As an optimizer, the DFP (Davidon-Fletcher-Powell) variable metric method is adopted with the golden section method in the ADS (Automated Design Synthesis) program[16].

The substitution of Eq. 9 into Eq. 6 yields

$$\begin{aligned}&\left([I]s^2+[C_m]s+[\Omega]\right)\{w_m(t)\}+[\Phi]^T\{\Theta\}V_p(t)=q\left([Q_0]+(b/U)[Q_1]s+(b/U)^2[Q_2]s^2\right.\\&\left.+[D]\left(\bar{s}[I]-(U/b)[R]\right)^{-1}[E]s\right)\{w_m(t)\}\end{aligned}. \tag{11}$$

Then the following state-space equations can be obtained from Eqs. 11 and 7:

$$\{\dot{x}\}=[A_s]\{x\}, \tag{12}$$

$$\{x\}=\left\{\{w_m\}^T,\{\dot{w}_m\}^T,\{p\}^T,\{V_p\}^T\right\}^T, \tag{13}$$

$$[A_s]=\begin{bmatrix}0 & [I] & 0 & 0\\ -[\overline{M}]^{-1}[\overline{K}] & -[\overline{M}]^{-1}[\overline{C}] & q[\overline{M}]^{-1}[D] & -[\overline{M}]^{-1}[\Phi]^T\{\Theta\}\\ 0 & [E] & (U/b)[R] & 0\\ 0 & (1/C')\{\Theta\}^T[\Phi] & 0 & 0\end{bmatrix}, \tag{14}$$

$$[\overline{M}]=[I]-q(b/U)^2[Q_2], \tag{15}$$

$$[\overline{C}]=[C_m]-q(b/U)[Q_1], \tag{16}$$

$$[\overline{K}]=[\Omega]-q[Q_0], \tag{17}$$

$$C'=\begin{cases}C_p+C_r & if \quad V_p=V_c\\ C_p-C_r & if \quad V_p=-V_c\\ C_p & if \quad |V_p|<V_c\end{cases}, \tag{18}$$

where the system matrix is denoted by A_s. The state vector is denoted by x, which consists of the modal displacements w_m, modal velocities $\dot{w}_m$, the augmented aerodynamic states p and voltage across the piezoelectric patch is denoted by V_p.

3. NUMERICAL RESULTS AND DISCUSSION

(1) Numerical model

In this research, aeroelastic flutter energy harvesting with a $[0_3/90]_s$ cantilevered laminated plate is examined. Cantilevered laminated plates with a piezoelectric element shown in Fig. 1 are employed, where a ply fiber angle is denoted by θ. Lead zirconate titanate (PZT) element is placed on the top surface of the plate. The material properties of lamina of carbon/epoxy composite and PZT element are shown in Tabs. 1 and 2. Here the in-plane stiffness and piezoelectric characteristics of piezoelectric material is assumed to be isotropic in this research. The four-node rectangular plate-bending element is employed in the present structural analysis based on the classical laminated plate theory, and 12×3 elements are used for the structural analysis. The sizes of PZT element are the same as that of a finite element in the structural analysis. On the other side, 8×6 elements are used for the aerodynamic analysis. The aerodynamic influence matrices are tabulated at 10 values of reduced frequency of 0.1, 0.111, 0.125, 0.143, 0.167, 0.2, 0.25, 0.333, 0.5 and 1, and the number of poles of transfer function r_{ir} is set to be 10. After the vibration analysis, a modal reduction is performed using

the lowest 10 modes to solve Eqs. 6 and 7, and then the Runge-Kutta method of the fourth order is adopted to integrate the state-space equations described as Eq. 12. Here the damping of the structure is neglected and the storage capacitor has a capacitance of 1.0 μF in this research.

(2) Results and discussion

Fig. 2 shows the aeroelastic characteristics of $[0_3/90]_s$ cantilevered laminated plates without piezoelectric patches. Figs. 2(a) and 2(b) correspond to the root loci with increasing free stream velocity and the flutter mode shape, respectively. It is found that the bending-torsional flutter due to coupling between the second and the first modes, which correspond to the first torsional and the first bending vibration modes, occurs at the speed U = 23.92 m/s.

Table 1: Material properties of CFRP.

E_{11} [GPa]	E_{22} [GPa]	G_{12} [GPa]	ν_{12}	ρ [kg/m^3]	Thickness [mm]
127.0	11.0	4.90	0.30	1541	0.125

Table 2: Material properties of PZT.

d_{31} [pm/V]	C_p [nF]	E [GPa]	ν	ρ [kg/m^3]	Thickness [mm]
-240	74.3	63.0	0.30	7800	0.25

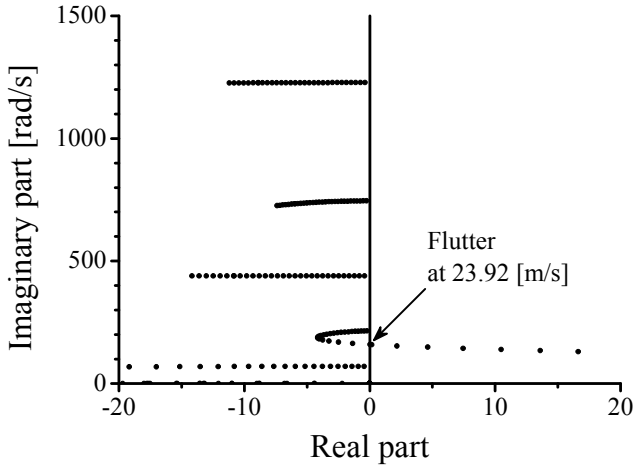

(a) Root loci with increasing free stream velocity.

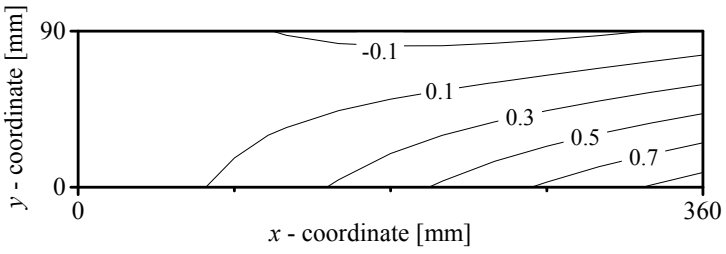

(b) Flutter mode shape.

Figure 2: Flutter characteristics.

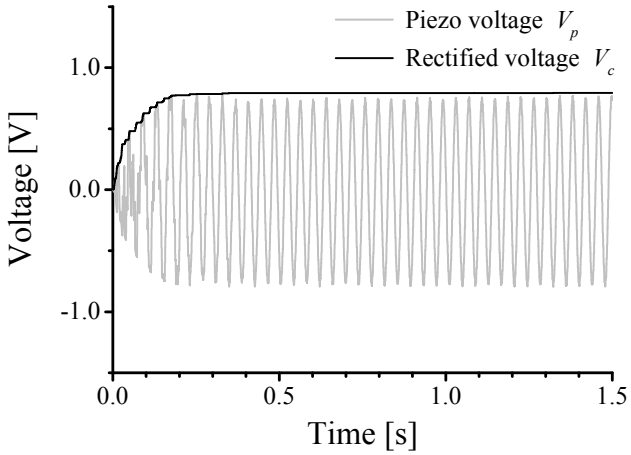

(a) Time histories of piezoelectric voltage and rectified voltage ($U = U_F = 24.56$ m/s).

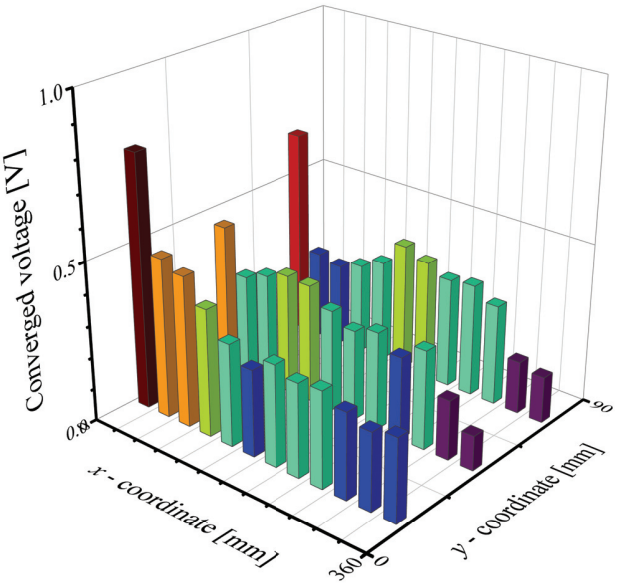

(b) Effect of location of piezoelectric patch on converged voltage in harvesting system.

Figure 3: Results of energy harvesting at flutter speed.

Fig. 3 shows the results of energy harvesting at the flutter speed $U = U_F$. Here the vibration of the plate is induced by sudden release of 1 mm initial deflection of the leading edge of the wing tip. Time histories of piezoelectric voltage and rectified voltage are shown in Fig. 3(a). As the aeroelastic vibration continued, the piezoelectric voltage and rectified voltage increased. Then the energy harvesting system reached a steady state and rectified voltage converged. Fig. 3(b) shows the effect of location of piezoelectric patch on converged voltage in the harvesting system, which corresponds to the flutter curvature mode shape. Fig. 4 shows the absolute values of a sum of plate bending curvature at the center of each finite element, which is obtained from Fig. 2(b). It is indicated that the optimal location of piezoelectric patch for energy harvesting can be determined based on the flutter curvature mode shape, by comparing with Fig. 3(b).

The effect of change of the operating condition on the result of energy harvesting is examined. Fig. 5 shows the effect of location of piezoelectric patch on converged voltage in the harvesting system at the speed $U = 0.9U_F$. It is found by comparing with Fig. 3(b) that the effect of location of piezoelectric patch on converged voltage is qualitatively same, although it becomes lower than that at the flutter speed $U = U_F$.

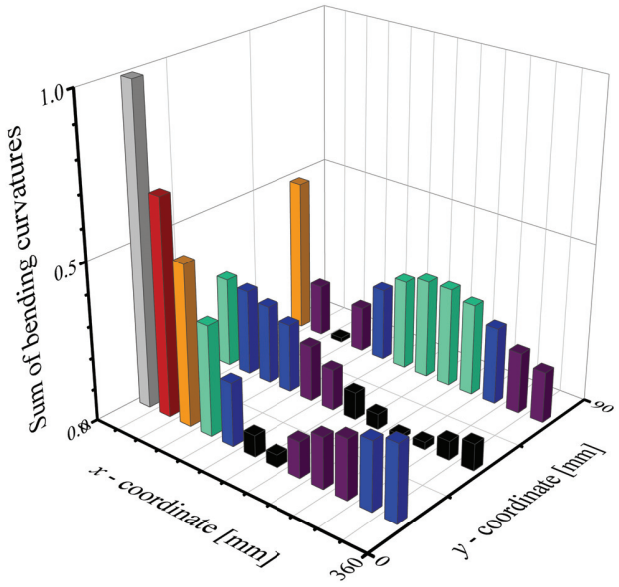

Figure 4: Absolute values of sum of plate bending curvatures.

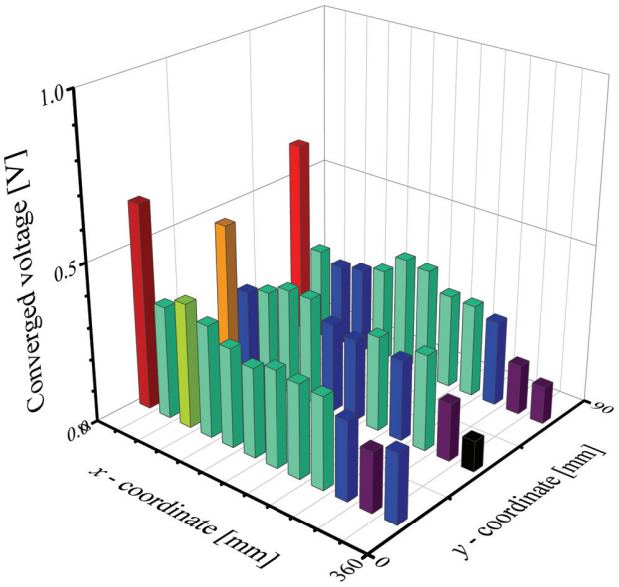

Figure 5: Effect of location of piezoelectric patch on converged voltage in harvesting system ($U = 0.9\ U_F$).

4. CONCLUSIONS

The present paper treats the piezoelectric energy harvesting from aeroelastic vibration with cantilevered laminated plates. It is indicated through the numerical examples that the optimal location of piezoelectric patch for energy harvesting can be determined based on the flutter curvature mode shape of the plate.

ACKNOWLEDGMENT

The author would like to thank Mr. I. Nakagawa and Mr. N. Kasahara, Department of Mechanical Systems Engineering, Shinshu University, for his support in the numerical simulation.

REFERENCES

1) De Marqui, C., Jr, Erturk, A. and Inman, D. J. : Piezoaeroelastic modeling and analysis of a generator wing with continuous and segmented electrodes, *J. Intell. Mater. Syst. Struct.*, Vol. 21, No. 10, pp. 983-993, 2010.
2) De Marqui, C., Jr., Vieira, W. G. R., Erturk, A. and Inman, D. J. : Modeling and analysis piezoelectric energy harvesting from aeroelastic vibrations using the doublet-lattice method, *J. Vib. Acoust.*, Vol. 133, No. 1, pp. 011003-1 - 011003-9, 2011.
3) Bryant, M. and Garcia, E. : Modeling and testing of a novel aeroelastic flutter energy harvester, *J. Vib. Acoust.*, Vol. 133, No. 1, pp. 011010-1 - 011010-11, 2011.
4) Dunnmon, J. A., Stanton, S. C., Mann, B. P. and Dowell, E. H. : Power extraction from aeroelastic limit cycle oscillations, *J. Fluids Struct.*, Vol. 27, No. 8, pp. 1182-1198, 2011.
5) Abdelkefi, A., Nayfeh, A. H. and Hajj, M. R. : Modeling and analysis of piezoelectric energy harvesters, *Nonlinear Dyn.*, Vol. 67, No. 2, pp. 925-939, 2012.
6) Hosking, N. S. and Sotoudeh, Z. : Energy harvesting from aeroelastic instabilities, AIAA-2016-0210, pp. 1-16, 2016.
7) Makihara, K. and Shimose, S. : Supersonic flutter utilization for effective energy-harvesting based on piezoelectric switching control, *Smart Mater. Res.*, Vol. 2012, pp. 181645-1 - 181645-10, 2012.
8) Isogai, K., Yamasaki, M. and Asaoka, T. : Application of CFD to design study of flutter-power-generation, NAL SP-57, pp. 106-111, 2003 (in Japanese).
9) Abiru, H. and Yoshitake, A. : Study on a flapping wing hydroelectric power generation system, *Trans. Jpn. Soc. Mech. Eng.* (*Ser. B*), Vol. 75, No. 758, pp. 2036-2041, 2009 (in Japanese).
10) Yan, Z. and Abdelkefi, A. : Nonlinear characterization of concurrent energy harvesting from galloping and base excitations, *Nonlinear Dyn.*, Vol. 77, No. 4, pp. 1171-1189, 2014.
11) Kameyama, M. : An efficient design approach for aeroelastic tailoring and control of composite plate wings, Ph. D. Thesis, 2006.
12) Shu, Y. C. and Lien, I. C. : Analysis of power output for piezoelectric energy harvesting systems, *Smart Mater. Struct.*, Vol. 15, No. 6, pp. 1499-1512, 2006.
13) Ueda, T. and Dowell, E. H. : A new solution method for lifting surfaces in subsonic flow, *AIAA J.*, Vol. 20, No. 3, pp. 348-355, 1982.
14) Harder, R. H. and Desmarais, R. N. : Interpolation using surface spline, *J. Aircr.*, Vol. 9, No. 2, pp. 189-191, 1972.
15) Karpel, M. : Time-domain aeroservoelastic modeling using weighted unsteady aerodynamic forces, *J. Guid. Control Dyn.*, Vol. 13, No. 1, pp. 30-37, 1990.
16) Vanderplaats, G. N. and Sugimoto, H. : A general-purpose optimization program for engineering design, *Comput. Struct.*, Vol. 24, No. 1, pp. 13-21, 1986.